iJRASET
International Journal For Research in Applied Science and Engineering Technology



# INTERNATIONAL JOURNAL FOR RESEARCH

IN APPLIED SCIENCE & ENGINEERING TECHNOLOGY

**Volume:** 14 **Issue:** X **Month of publication:** October 2026

**DOI:** https://doi.org/10.22214/ijraset.2026.85316

www.ijraset.com

Call: 08813907089 | E-mail ID: ijraset@gmail.com

International Journal for Research in Applied Science & Engineering Technology (IJRASET)
*ISSN: 2321-9653; IC Value: 45.98; SJ Impact Factor: 7.538*
*Volume 14 Issue X Oct 2026- Available at www.ijraset.com*

# PELAGIX: An Intelligent Decentralized Framework for Verified Quantification and Transparent Trading of Blue Carbon Assets

Sanket Jaiswal[1], Satish Patel[2], Soham Nimje[3], Prachi Jain[4], Spandan Karandikar[5], Srujan Barshe[6]
*School of Engineering and Technology, Computer Science & Engineering, G H Raisoni University, Amravati, India*

***Abstract:*** ***Mangrove carbon assessments require spatially explicit methods whose assumptions, data support, and verification status remain traceable. This study presents an integrated workflow for operational mangrove mapping, modeled above-ground carbon (AGC) estimation, complementary carbon accounting, parameter sensitivity, and a prototype digital measurement, reporting, and verification (MRV) provenance layer for a Sundarbans area bounded by approximately 88.10–89.10°E and 21.50–22.35°N. Sentinel-2 surface-reflectance observations from 1 January to 30 April 2023 were cloud-screened, median composited, and used to calculate NDVI; NDVI > 0.4 defined the operational mangrove mask. The supplied Google Earth Engine workflow quality-screened GEDI monthly rh100, median-composited it, applied its original rh100/100 transformation, and filled unobserved structural values using 15× NDVI. Biomass and carbon were modeled as AGB = H× NDVI× 10.5 and AGC = 0.47× AGB. The retained raster footprint contains 15,793,243 mangrove cells (157,932.43 ha under the nominal 0.01 ha-per-cell convention). Mean AGC density was 2.8060 t C ha$^{-1}$ (median 2.7935; standard deviation 0.6325), with total modeled AGC of 443,164.99 t C and derived AGB of 942,904.24 t. A separate InVEST baseline reports 409,383 t C. Combined variation of the project-specific AGB coefficient and carbon fraction produced 343,486.54–550,027.47 t C (-22.49% to +24.11%); this is parameter sensitivity, not a confidence interval. GEE and InVEST outputs are complementary, non-equivalent model results. The prototype demonstrates evidence handling and digital provenance workflows, not carbon-credit certification or independent verification. No independent field validation was available, and reported values represent modeled above-ground carbon rather than total ecosystem carbon.***

***Keywords: mangrove; blue carbon; Sentinel-2; GEDI; above-ground carbon; Google Earth Engine; InVEST; digital MRV; provenance.***

## I. INTRODUCTION

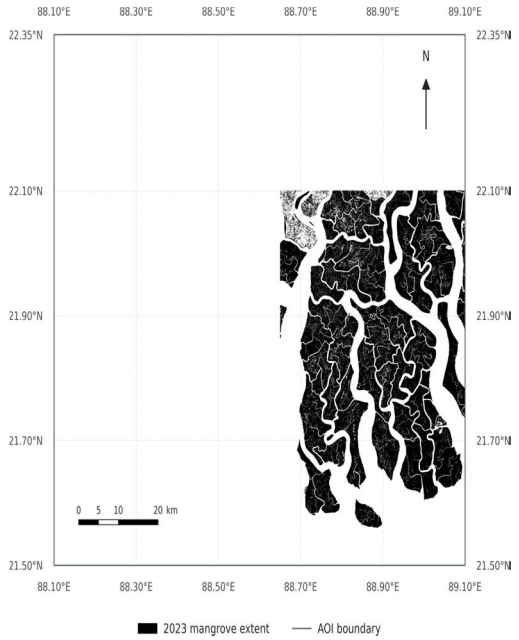
Mangroves support coastal habitat, fisheries, shoreline processes, and substantial carbon stocks. Their climate significance includes both stored carbon and the potential emissions associated with ecosystem loss; defensible assessment therefore requires clearly defined carbon pools and careful interpretation of stock estimates [1–3]. Mangrove blue carbon includes above-ground and below-ground biomass, dead organic matter, and soil carbon. A remotely modeled above-ground carbon (AGC) quantity alone is not a total ecosystem-carbon inventory, and its interpretation depends on measurement design and the evidence available for calibration and validation [4, 5].

Satellite observations and geographic information systems extend spatial coverage in coastal landscapes where field access can be difficult. Sentinel-2 multispectral imagery supports vegetation characterization and land monitoring [6]; GEDI waveform lidar provides canopy-structure observations at sampled locations rather than continuous measurement at every map cell [7]. Integration of optical and structural data can support spatial modeling, but image resolution by itself does not demonstrate classification or carbon-estimation accuracy. Reviews of mangrove remote-sensing assessments highlight continuing challenges in validation, pool completeness, and comparability [8]. Regional Sundarbans biomass studies provide context but do not calibrate the project-specific equation used here [9, 10].

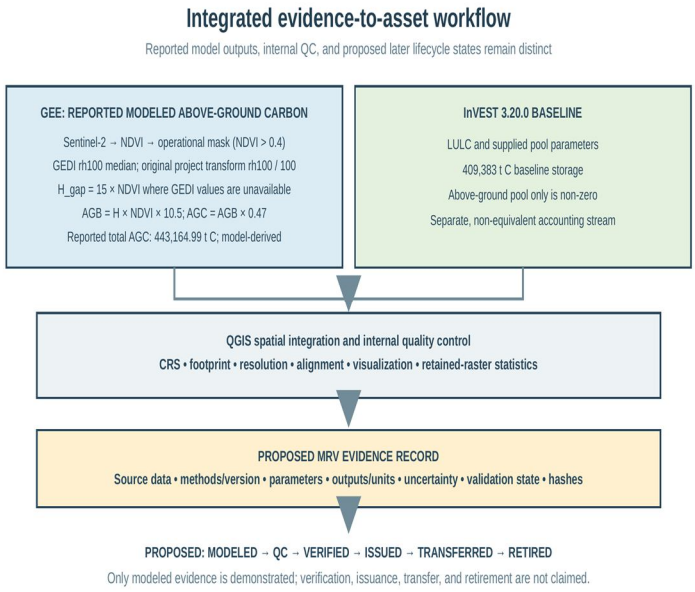
A further challenge is traceability: a reported raster total can become detached from its spatial footprint, equations, parameters, and validation status. Digital MRV and provenance systems may organize evidence and record processing history, but automation does not independently establish ecological validity [11]. Blockchain and digital-carbon research discusses potential provenance and lifecycle functions alongside governance and interoperability constraints [12–15].

©IJRASET: All Rights are Reserved 

This study documents a workflow connecting Sentinel-2 and GEDI processing, modeled AGC, a separate InVEST baseline, parameter sensitivity, geospatial quality control, and a conceptual digital-MRV/provenance architecture for the Sundarbans. Its contribution is the integration of these components while explicitly distinguishing modeled carbon, independently verified environmental quantities, and digital-asset lifecycle states. It does not claim field validation, credit issuance, or a market transaction.




(a) Analytical AOI and quantitative footprint.




(b) Integrated evidence-to-asset framework.

Figure 1: Study setting and framework. Quantitative outputs cover a smaller extent than the analytical AOI; verification and asset lifecycle states are proposed rather than demonstrated.

## II. MATERIALS AND METHODS

### A. *Study Area*

The analytical area of interest (AOI) is bounded by 88.10–89.10°E and 21.50–22.35°N. The supplied quantitative 2023 GeoTIFF products cover a smaller footprint, approximately 88.649974–89.100030°E and 21.549955–22.100173°N, in EPSG:4326 / WGS 84. The reported raster statistics therefore describe the retained product footprint, not the full analytical AOI. The supplied workflow applies a nominal area of 0.01 ha per 10 m cell; this implemented convention is retained without substituting a geodesic-area calculation.

### B. *Data Sources and Software*

Sentinel-2 surface reflectance, GEDI structure, supplied quantitative rasters, and the InVEST baseline form the principal inputs (Table 1). Google Earth Engine (GEE) supported filtering, compositing, and raster modeling [16]; QGIS supported projection handling, spatial inspection, visualization, and quality control. InVEST 3.20.0 supplied a separate land-use/land-cover (LULC)-based carbon-storage estimate [17].

### C. *Sentinel-2 Preprocessing*

Sentinel-2 imagery from 1 January through 30 April 2023 was filtered to the AOI and image-level cloud percentage below 20%. QA60 bits 10 (opaque cloud) and 11 (cirrus) were masked. Surface-reflectance values were scaled as $\rho_b = DN_b/10000$, and retained observations were median-composited.

Table 1: Datasets, software, and principal processing parameters.

| Component | Source | Period/domain | Role and processing |
|---|---|---|---|
| Sentinel-2 | COPERNICUS/S2_SR_HARMONIZED | 2023-01-01–2023-04-30; AOI | Image cloud percentage < 20%; QA60 bits 10 and 11 masked; reflectance divided by 10,000; median composite; B8 and B4 used for NDVI. |
| GEDI | LARSE/GEDI/GEDI02_A_002_MONTHLY | Monthly product over AOI | Select rh100; quality_flag=1; degrade_flag=0; median composite; original project transformation rh100/100. |
| AOI / outputs | Analytical AOI and two supplied 2023 GeoTIFFs | AOI bounds in text; EPSG:4326 | Output footprint is smaller than AOI; retained raster has 30,686,250 cells and nominal 0.01 ha per cell. |
| InVEST | InVEST Carbon Storage and Sequestration 3.20.0 | Supplied LULC and pool table | Separate class-based baseline; only above-ground biomass is non-zero in the supplied pool configuration. |
| Platforms | GEE; QGIS | Project workflow | GEE processing and exports; QGIS spatial inspection and internal QC, not independent carbon validation. |

### *D. NDVI-Based Mangrove Mask*

NDVI was calculated from near-infrared band B8 and red band B4:

$$\mathrm{NDVI} = \frac{B8 - B4}{B8 + B4}. \qquad (1)$$

The operational mangrove mask was defined as $M = 1$ where NDVI > 0.4 and $M = 0$ otherwise. This project-specific threshold is not treated as a universal mangrove classifier.

### *E. GEDI Canopy-Height Processing*

The workflow selected rh100 from LARSE/GEDI/GEDI02_A_002_MONTHLY, retained observations with quality_flag=1 and degrade_flag=0, and median-composited the quality-screened observations. It then applied the original project transformation $H_{\mathrm{GEDI}}$ = rh100/100. This is reported as implemented, not as a universal unit conversion. Unobserved structural cells were filled according to $H_{\mathrm{gap}} = 15 \times \mathrm{NDVI}$, equivalent to the supplied unmask operation. No separate GEDI support mask was retained in the quantitative outputs, so observed and filled-cell contributions cannot be separately quantified.

### *F. Above-Ground Biomass Estimation*

Above-ground biomass density was modeled as

$$\mathrm{AGB} = H_{\mathrm{estimated}} \times \mathrm{NDVI} \times 10.5, \qquad (2)$$

where 10.5 is the project-specific empirical coefficient; independent calibration evidence was unavailable.

### *G. Above-Ground Carbon Estimation*

Modeled above-ground carbon density was calculated as

$$\mathrm{AGC} = 0.47 \times \mathrm{AGB}, \qquad (3)$$

where 0.47 is the project-specified biomass-to-carbon fraction, not a universal or IPCC-mandated mangrove constant. The carbon quantity per cell follows the implementation $C_{\mathrm{pixel}} = \mathrm{AGC} \times 0.01$, using the nominal 0.01 ha pixel area. These equations represent above-ground pools only.

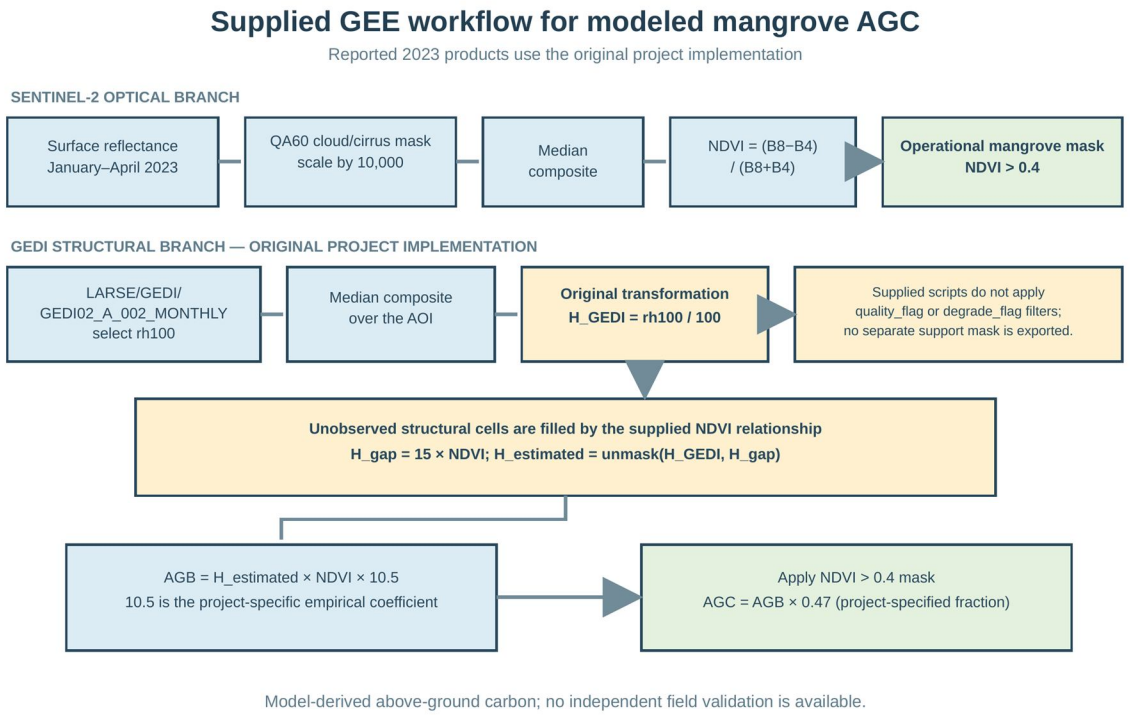



Figure 2: Remote-sensing workflow from Sentinel-2 preprocessing and NDVI mapping through GEDI quality screening, the implemented height transformation and gap filling, and modeled AGB and AGC. No separate GEDI support mask is retained.

### *H. InVEST Carbon Storage Estimation*

The supplied InVEST 3.20.0 result was retained as a separate LULC-based baseline. It reports 409,383 t C using the supplied biophysical table, in which above-ground biomass is the only non-zero carbon pool. The result is not a field measurement, a full four-pool inventory, or an independent validation of the GEE estimate.

### *I. Sensitivity Analysis*

Sensitivity scenarios vary the AGB coefficient across 8.5, 10.5, and 12.5 and the biomass-to-carbon fraction across 0.45, 0.47, and 0.49. Combined scenarios were scaled from the reported baseline $C_0$ = 443,164.99 t C as

$$C_{B,f} = C_0 \frac{B}{10.5} \frac{f}{0.47}, \qquad (4)$$

where $B$ and $f$ are the tested coefficient and carbon fraction. The resulting range is parameter sensitivity, not a confidence interval, prediction interval, or complete uncertainty assessment. Threshold alternatives and footprint-wide gap-fill scenarios could not be calculated from the retained products.

### *J. Digital MRV and Provenance Architecture*

The conceptual evidence record links the AOI and actual output footprint, coordinate reference system and raster dimensions, observation period, source datasets, processing version, equations and parameters, quality masks, output units, sensitivity scenarios, validation status, and evidence identifiers. The proposed lifecycle distinguishes MODELED, QC, VERIFIED, ISSUED, TRANSFERRED, and RETIRED. Blockchain or digital provenance can preserve identifiers and processing records, but does not itself establish scientific accuracy, eligibility, ownership, independent verification, additionality, permanence, or registry approval.

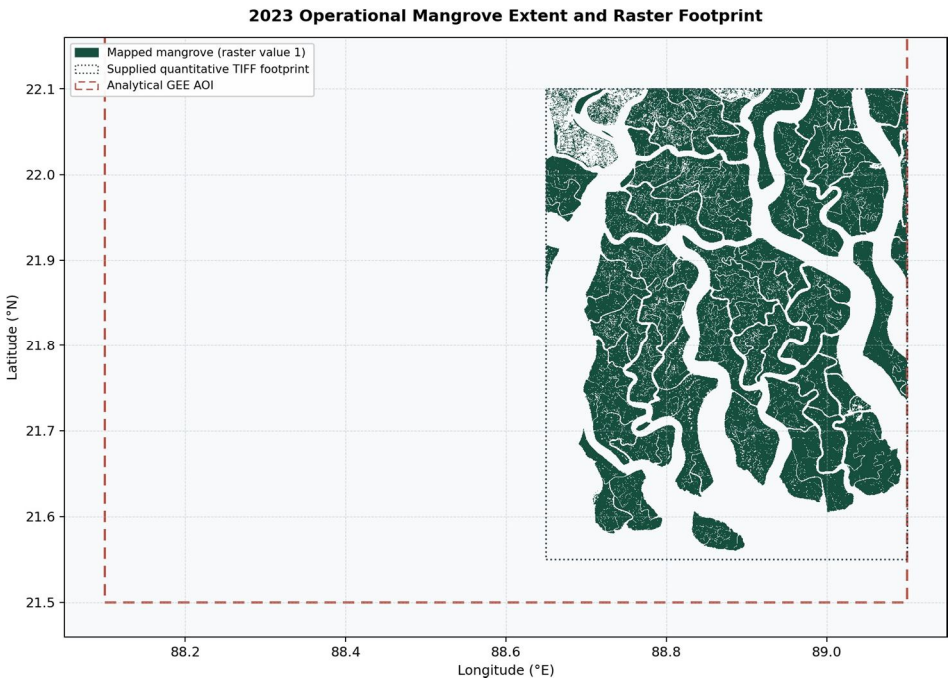



Figure 3: Mapped 2023 operational mangrove extent from the supplied binary raster (1 = mangrove; 0 = other), based on NDVI > 0.4. The classification is not independently field-validated.

### *K. Prototype Implementation*

The BlueChain prototype demonstrates project registration and boundary entry, carbon-analysis presentation, verifier review, project-status management, metadata/IPFS handling, blockchain transaction interaction, and digital-asset/NFT representation. The interfaces demonstrate workflow functionality only. Their displayed carbon values are demonstration/test outputs and are not used in the authoritative Sundarbans-wide results.

## III. RESULTS AND DISCUSSION

### *A. Mangrove Extent and Spatial Carbon Estimation*

The retained quantitative grid contains 30,686,250 cells. Of these, 15,793,243 are classified as mangrove and 14,893,007 as non-mangrove, giving a mangrove-cell proportion of 51.4668%. Applying the project's nominal 0.01 ha per cell yields a mapped operational extent of 157,932.43 ha (1,579.32 $km^2$). This describes the supplied raster footprint, not the full AOI, and preserves the implemented area convention.

### *B. Carbon-Density Characteristics*

Mean modeled AGC density is 2.8060 t C $ha^{-1}$, median 2.7935 t C $ha^{-1}$, and standard deviation 0.6325 t C $ha^{-1}$. The reported minimum is 0.1606 and maximum is 16.0198 t C $ha^{-1}$. Total modeled AGC is 443,164.99 t C. Dividing by the project-specified 0.47 carbon fraction gives derived total AGB of 942,904.24 t, with mean AGB density 5.9703 t $ha^{-1}$ (Table 2). These are model-derived values, not field measurements. Their variation describes the modeled output; it does not establish ecological accuracy or local ecological causes.

### *C. Comparison with InVEST Carbon Storage*

InVEST reports baseline carbon storage of 409,383 t C. This is complementary to, rather than directly equivalent to, the GEE-derived 443,164.99 t C modeled AGC (Table 3). GEE produces continuous modeled AGC using the height/NDVI equations and nominal cell-area aggregation; InVEST assigns supplied carbon-pool values to LULC classes. The estimates differ in framework, spatial support, pool representation, and parameterization. Their numerical difference must not be interpreted as model accuracy or validation.

©IJRASET: All Rights are Reserved | SJ Impact Factor 7.538 | ISRA Journal Impact Factor 7.894 |

Table 2: Principal modeled carbon results for the retained raster footprint.

| Metric | Reported value |
|---|---|
| Total raster cells | 30,686,250 |
| Mapped mangrove cells | 15,793,243 |
| Mangrove-cell proportion | 51.4668% |
| Mapped mangrove area | 157,932.43 ha |
| Mean modeled AGC density | 2.8060 t C $ha^{-1}$ |
| Median modeled AGC density | 2.7935 t C $ha^{-1}$ |
| Standard deviation | 0.6325 t C $ha^{-1}$ |
| Minimum modeled AGC density | 0.1606 t C $ha^{-1}$ |
| Maximum modeled AGC density | 16.0198 t C $ha^{-1}$ |
| Total modeled AGC | 443,164.99 t C |
| Mean AGB density | 5.9703 t $ha^{-1}$ |
| Total modeled AGB | 942,904.24 t |

Table 3: GEE-derived AGC and InVEST baseline carbon storage.

| Framework | Carbon (t C) | Scope and interpretation |
|---|---|---|
| GEE-derived AGC | 443,164.99 | Modeled above-ground carbon from the supplied Sentinel-2/GEDI workflow; nominal area aggregation. |
| InVEST baseline | 409,383 | LULC-based baseline under supplied pool parameters; only the above-ground pool is non-zero. |

Note: These estimates use different modeling frameworks and are complementary rather than directly equivalent validation measurements.

### *D. Sensitivity Analysis*

Combined parameter scenarios span 343,486.54–550,027.47 t C, or −22.49% to +24.11% relative to baseline (Table 4). This range demonstrates sensitivity to the selected empirical coefficient and carbon fraction. It does not encompass classification, structural-data support, gap filling, model form, or spatial-processing uncertainty and is not a statistical interval.

### *E. Digital MRV and Provenance Implications*

The framework links modeled quantities to the data period, footprint, equations, parameters, sensitivity, and validation status. The provenance layer is intended to support evidence organization and lifecycle traceability. A modeled stock is distinct from a verified environmental quantity, and both are distinct from an issued or tradable digital asset.

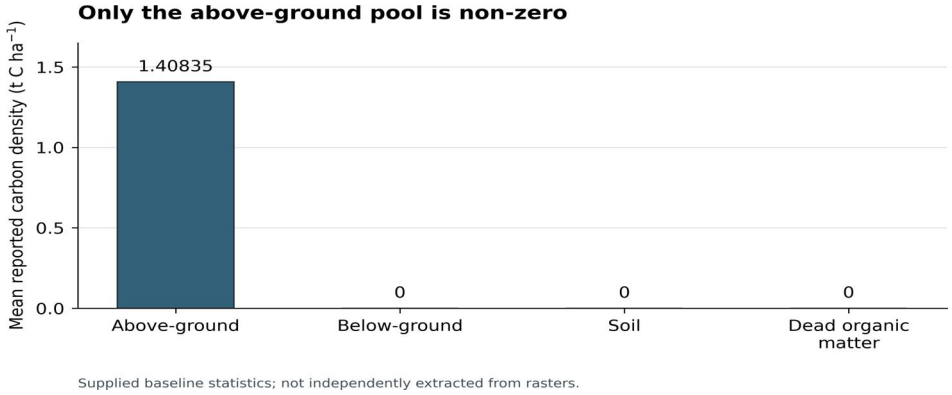



Figure 4: Reported InVEST pool contribution under the supplied biophysical parameterization. Zero values indicate the supplied configuration, not ecological absence of the corresponding pools.

Table 4: Combined parameter sensitivity relative to the reported baseline.

| Scenario | Total modeled AGC (t C) | Difference from baseline |
|---|---|---|
| Lower (coefficient 8.5; fraction 0.45) | 343,486.54 | −22.49% |
| Baseline (coefficient 10.5; fraction 0.47) | 443,164.99 | 0.00% |
| Upper (coefficient 12.5; fraction 0.49) | 550,027.47 | +24.11% |

### *F. Prototype Implementation*

Figure 6 consolidates the six prototype screenshots. They demonstrate registration, analysis presentation, verifier review, transaction request, and digital representation. The analysis screen displays approximately 1,235.62 tonnes C; this is a demonstration/test output, not the authoritative Sundarbans-wide estimate reported here. A wallet request or minting confirmation is not evidence of an actual carbon-market transaction, external certification, or legal ownership.

## IV. LIMITATIONS AND IMPLICATIONS

No independent field validation was available; no RMSE, MAE, $R^2$, classification accuracy, or field-calibrated performance statistic is therefore reported. The AGB relationship uses the project-specific coefficient 10.5, and 0.47 is a project-specified carbon fraction. NDVI > 0.4 is an operational threshold, not a validated universal classifier. The empirical 15× NDVI relationship fills missing structural values, but the quantitative outputs do not retain a separate GEDI support mask. The supplied raster footprint is smaller than the analytical AOI, and area aggregation uses the nominal 0.01 ha-per-cell convention in EPSG:4326.

GEE and InVEST arise from different frameworks, extents, pool scopes, and parameters; their difference is not validation. Sensitivity testing varies two parameters and is not a full statistical uncertainty analysis. No quantitative 2019–2023 carbon change, sequestration rate, or carbon-credit quantity is established. The digital MRV/provenance architecture and prototype are conceptual/software demonstrations. Blockchain technology cannot independently establish ecological validity, additionality, permanence, eligibility, external verification, legal ownership, registry acceptance, or carbon-credit certification. Future deployment would require separate observed and gap-filled layers, representative independent field measurements, explicit support and uncertainty information, appropriate pool data, and external review under applicable MRV rules.

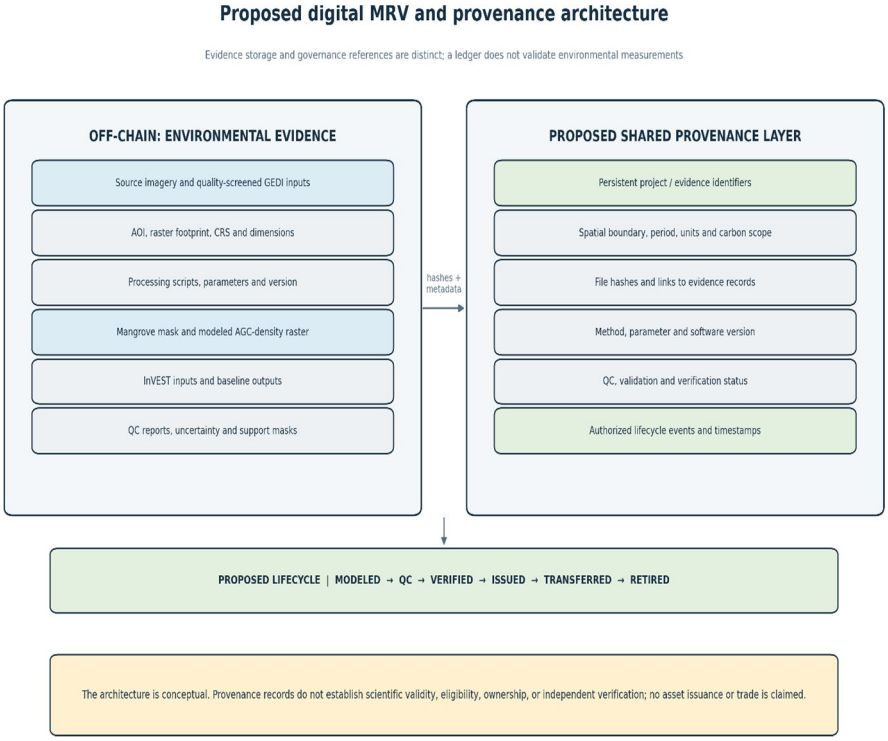
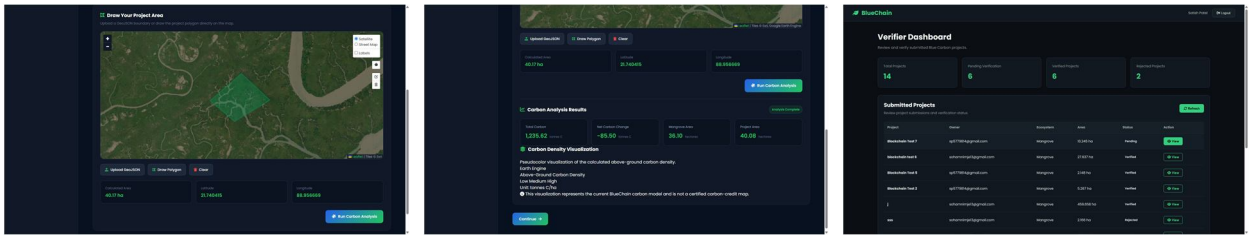
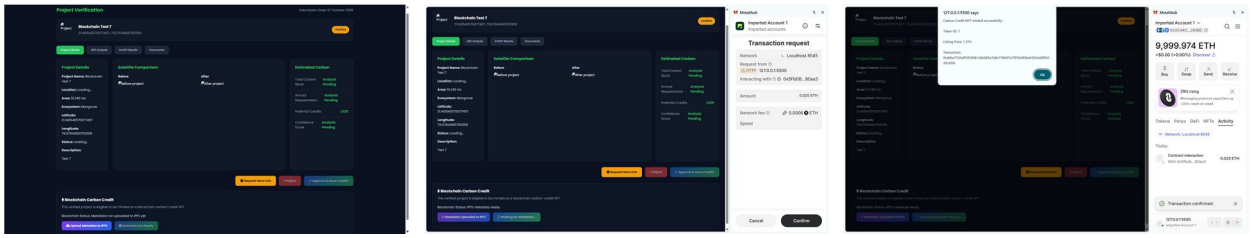



Figure 5: Proposed MRV provenance architecture linking off-chain environmental evidence with identifiers, metadata, integrity hashes, quality-control and verification status, and lifecycle records. The architecture is conceptual and does not independently establish validity or verification.



**(a)** Registration/boundary. **(b)** Analysis interface. **(c)** Verifier dashboard.



**(d)** Project/blockchain view. **(e)** Wallet request. **(f)** Prototype mint confirmation.

Figure 6: Prototype implementation screens for registration, analysis, review, and digital-asset workflow. Interface values and transaction states are demonstration/test outputs, not authoritative Sundarbans-wide estimates, external verification, or certified carbon credits.

## V. CONCLUSION

This study documents a spatially explicit workflow combining 2023 Sentinel-2 vegetation information, quality-screened GEDI rh100, project-defined height processing and gap filling, modeled AGB and AGC, a separate InVEST baseline, parameter sensitivity, and a proposed evidence-centric digital-MRV layer. For the retained raster footprint, mapped mangrove extent is 157,932.43 ha and total modeled AGC is 443,164.99 t C; InVEST separately reports 409,383 t C under its supplied LULC and pool parameters. Combined parameter scenarios span 343,486.54–550,027.47 t C, demonstrating sensitivity rather than statistical uncertainty. These values represent modeled above-ground carbon and are not independently field-validated or equivalent to total ecosystem carbon. The prototype demonstrates evidence handling and provenance, not certified credits or independently verified environmental quantities. Field validation, stronger support and uncertainty records, and external verification remain necessary before any application to credit issuance or trade.

## REFERENCES

[1] D. C. Donato, J. B. Kauffman, D. Murdiyarso, S. Kurnianto, M. Stidham, and M. Kanninen, "Mangroves among the most carbon-rich forests in the tropics," Nature Geoscience, vol. 4, pp. 293–297, 2011, doi: 10.1038/ngeo1123.

[2] E. McLeod, G. L. Chmura, S. Bouillon, R. Salm, M. Björk, C. M. Duarte, C. E. Lovelock, W. H. Schlesinger, and B. R. Silliman, "A blueprint for blue carbon: Toward an improved understanding of the role of vegetated coastal habitats in sequestering $CO_2$," Frontiers in Ecology and the Environment, vol. 9, no. 10, pp. 552–560, 2011, doi: 10.1890/110004.

[3] P. I. Macreadie, M. D. P. Costa, T. B. Atwood, D. A. Friess, J. J. Kelleway, H. Kennedy, C. E. Lovelock, O. Serrano, and C. M. Duarte, "Blue carbon as a natural climate solution," Nature Reviews Earth & Environment, vol. 2, pp. 826–839, 2021, doi: 10.1038/s43017-021-00224-1.

[4] D. A. Friess, Z. I. Shribman, M. Stankovic, N. Iram, M. M. Baustian, and C. J. Ewers Lewis, "Restoring blue carbon ecosystems," Cambridge Prisms: Coastal Futures, vol. 2, art. e9, 2024, doi: 10.1017/cft.2024.9.

[5] M. M. Moritsch, M. A. Young, P. Carnell, P. I. Macreadie, C. E. Lovelock, E. Nicholson, P. T. Raimondi, L. M. Wedding, and D. Ierodiaconou, "Estimating blue carbon sequestration under coastal management scenarios," Science of the Total Environment, vol. 777, art. 145962, 2021, doi: 10.1016/j.scitotenv.2021.145962.

[6] B. J. Fest, S. E. Swearer, and S. K. Arndt, "A review of sediment carbon sampling methods in mangroves and their broader impacts on stock estimates for blue carbon ecosystems," Science of the Total Environment, vol. 816, art. 151618, 2022, doi: 10.1016/j.scitotenv.2021.151618.

[7] A. Dutta Roy, P. S. Pitumpe Arachchige, M. S. Watt, A. Kale, M. Davies, J. E. Heng, et al., "Remote sensing-based mangrove blue carbon assessment in the Asia-Pacific: A systematic review," Science of the Total Environment, vol. 938, art. 173270, 2024, doi: 10.1016/j.scitotenv.2024.173270.

[8] P. Potapov, X. Li, A. Hernandez-Serna, A. Tyukavina, M. C. Hansen, A. Kommareddy, A. H. Pickens, S. Turubanova, H. Tang, C. A. Silva, J. Armston, R. Dubayah, J. B. Blair, and M. Hofton, "Mapping global forest canopy height through integration of GEDI and Landsat data," Remote Sensing of Environment, vol. 253, art. 112165, 2021, doi: 10.1016/j.rse.2020.112165.

[9] N. Gorelick, M. Hancher, M. Dixon, S. Ilyushchenko, D. Thau, and R. Moore, "Google Earth Engine: Planetary-scale geospatial analysis for everyone," Remote Sensing of Environment, vol. 202, pp. 18–27, 2017, doi: 10.1016/j.rse.2017.06.031.

[10] M. Drusch, U. Del Bello, S. Carlier, O. Colin, V. Fernandez, F. Gascon, B. Hoersch, C. Isola, F. Laberinti, F. Martimort, A. Meygret, F. Spoto, O. Sy, F. Marchese, and P. Bargellini, "Sentinel-2: ESA's optical high-resolution mission for GMES operational services," Remote Sensing of Environment, vol. 120, pp. 25–36, 2012, doi: 10.1016/j.rse.2011.11.026.

[11] R. Dubayah, J. B. Blair, S. Goetz, L. Fatoyinbo, M. Hansen, S. Healey, M. Hofton, G. Hurtt, J. Kellner, S. Luthcke, J. Armston, H. Tang, L. Duncanson, S. Hancock, P. Jantz, S. Marselis, P. L. Patterson, W. Qi, and C. E. Silva, "The Global Ecosystem Dynamics Investigation: High-resolution laser ranging of the Earth's forests and topography," Science of Remote Sensing, vol. 1, art. 100002, 2020, doi: 10.1016/j.srs.2020.100002.

[12] T. Hiraishi, T. Krug, K. Tanabe, N. Srivastava, J. Baasansuren, M. Fukuda, and T. G. Troxler, Eds., 2013 Supplement to the 2006 IPCC Guidelines for National Greenhouse Gas Inventories: Wetlands. Switzerland: Intergovernmental Panel on Climate Change, 2014.

[13] Natural Capital Alliance, InVEST 3.20.0. 2026, doi: 10.60793/natcap-invest-3.20.0.

[14] Verra, "VM0033 Methodology for Tidal Wetland and Seagrass Restoration," ver. 2.1, active Sep. 4, 2023. [Online]. Available: https://verra.org/methodologies/vm0033-methodology-for-tidal-wetland-and-seagrass-restoration-v2-1/

[15] M.-F. Körner, C. Leinauer, T. Ströher, and J. Strüker, "Digital measuring, reporting, and verification (dMRV) for decarbonization," Business & Information Systems Engineering, vol. 67, pp. 753–765, 2025, doi: 10.1007/s12599-025-00953-3.

[16] A. Vilkov and G. Tian, "Blockchain's scope and purpose in carbon markets: A systematic literature review," Sustainability, vol. 15, no. 11, art. 8495, 2023, doi: 10.3390/su15118495.

[17] A. L. C. Merlo, D. S. Mendonça, J. Santos, S. T. Carvalho, R. Guerra, and D. Brandão, "Blockchain for the carbon market: A literature review," Discover Environment, vol. 3, art. 68, 2025, doi: 10.1007/s44274-025-00260-4.

[18] S. Jaffer, M. W. Dales, P. Ferris, T. Swinfield, D. Sorensen, R. Message, S. Keshav, and A. Madhavapeddy, "Global, robust and comparable digital carbon assets," in Proc. IEEE Int. Conf. Blockchain and Cryptocurrency (ICBC), 2024, pp. 305–306, doi: 10.1109/ICBC59979.2024.10634343.

[19] J. Woo, R. Fatima, C. J. Kibert, R. E. Newman, Y. Tian, and R. S. Srinivasan, "Applying blockchain technology for building energy performance measurement, reporting, and verification (MRV) and the carbon credit market: A review of the literature," Building and Environment, vol. 205, art. 108199, 2021, doi: 10.1016/j.buildenv.2021.108199.

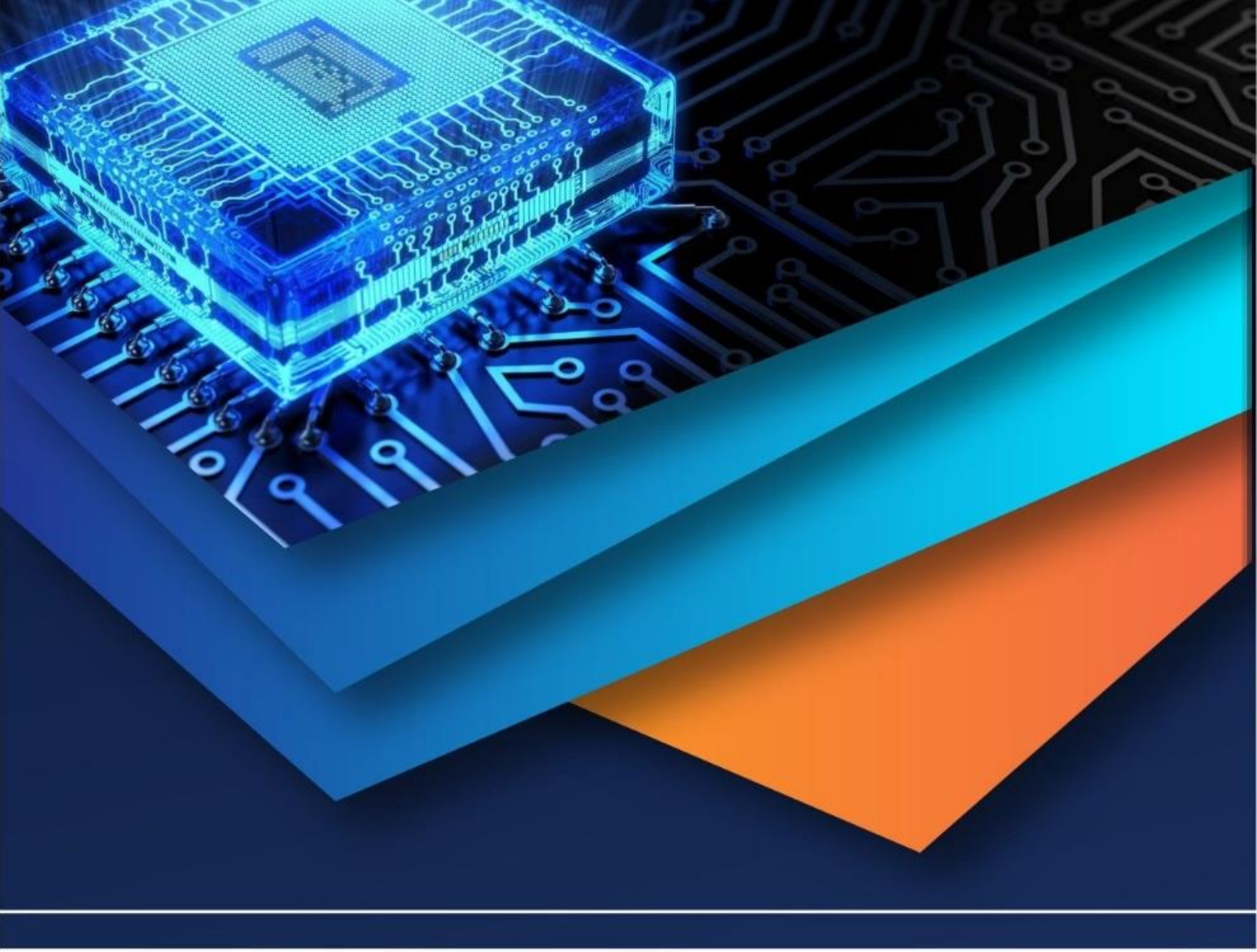
[20] J. Ding and Y. Lu, "A hybrid IoT-Hadoop-blockchain architecture for decentralized MRV and carbon data governance," Frontiers in Climate, vol. 8, art. 1776972, 2026, doi: 10.3389/fclim.2026.1776972.

[21] M. Jia, Z. Wang, D. Mao, C. Ren, K. Song, C. Zhao, C. Wang, X. Xiao, and Y. Wang, "Mapping global distribution of mangrove forests at 10-m resolution," Science Bulletin, vol. 68, no. 12, pp. 1306–1316, 2023, doi: 10.1016/j.scib.2023.05.004.

[22] J. B. Kauffman and D. Donato, "Protocols for the measurement, monitoring and reporting of structure, biomass and carbon stocks in mangrove forests," CIFOR Working Paper 86, Center for International Forestry Research, Bogor, Indonesia, 2012, doi: 10.17528/cifor/003749.

[23] A. Mitra, K. Sengupta, and K. Banerjee, "Standing biomass and carbon storage of above-ground structures in dominant mangrove trees in the Sundarbans," Forest Ecology and Management, vol. 261, no. 7, pp. 1325–1335, 2011, doi: 10.1016/j.foreco.2011.01.012.

[24] N. Das, A. Mondal, N. C. Saha, S. Ghosh, and S. Mandal, "Decadal loss of above-ground biomass and subsequent potential $CO_2$ emission from the Sundarbans mangrove ecosystem, India," Acta Ecologica Sinica, vol. 43, no. 3, pp. 452–458, 2023, doi: 10.1016/j.chnaes.2021.11.002.



10.22214/IJRASET

45.98

IMPACT FACTOR: 7.129

IMPACT FACTOR: 7.429

# INTERNATIONAL JOURNAL FOR RESEARCH

IN APPLIED SCIENCE & ENGINEERING TECHNOLOGY

Call : 08813907089 (24*7 Support on Whatsapp)